International Journal of Engineering, Mathematical and Physical Sciences
ISSN: 2517-9934
Vol:6, No:11, 2012

Shell Closures in Exotic Nuclei

G. Saxena, D. Singh, and M. Kaushik,

Abstract—Inspired by the recent experiments [1]-[3] indicating unusual doubly magic nucleus ^{24}O which lies just at the neutron drip-line and encouraged by the success of our relativistic mean-field (RMF) plus state dependent BCS approach for the description of the ground state properties of the drip-line nuclei [23]-[27], we have further employed this approach, across the entire periodic table, to explore the unusual shell closures in exotic nuclei. In our RMF+BCS approach the single particle continuum corresponding to the RMF is replaced by a set of discrete positive energy states for the calculations of pairing energy. Detailed analysis of the single particle spectrum, pairing energies and densities of the nuclei predict the unusual proton shell closures at Z = 6, 14, 16, 34, and unusual neutron shell closures at N = 6, 14, 16, 34, 40, 70, 112.

Keywords—Relativistic Mean Field theory, Magic Nucleus, Si isotopes, Shell Closure.

I. Introduction

EXPERIMENTAL and theoretical studies of exotic nuclei with extreme isospin values constitute one of the most active current areas of research in nuclear physics. Experiments [1]-[5] with radioactive nuclear beams provide the opportunity to study very short-lived nuclei with large |N-Z| value. Especially, the neutron rich nuclei with unusually large isospin value are known to exhibit several interesting features. Obviously for such nuclei, the role of continuum states and their coupling to the bound states become exceedingly important, especially for the pairing energy contribution to the total binding energy of the system. In recent experiments with radioactive nuclear beams (RNB), disappearance of traditional magic numbers and appearance of new magic numbers have been observed in nuclei with exotic isospin ratios [4], [5].

More recently, it has been demonstrated in two independent experiments [2], [3] that ^{24}O, the heaviest isotope of oxygen with neutron number N = 16, is a doubly magic nucleus. Both experiments used secondary beams to probe the properties of ^{24}O. They started from a high-energy primary beam of the calcium isotope ^{48}Ca, which was made to interact with a beryllium target to produce a multitude of nuclear fragments. Fragment separators were then used to identify and select the species of interest, collect them into a beam (the secondary beam) and send them on to a reaction target.

Theoretical descriptions of drip line nuclei in terms of a few body model or clusters [6], [7], shell model [8], [9] and mean field theories, both nonrelativistic [10], [11] as well as relativistic mean field (RMF) [12]– [29] have been well received. The advantage of the RMF approach is that it provides the spin-orbit interaction in the entire mass region, which is consistent with the nuclear density [16]. This indeed has been found to be very important for the study of unstable nuclei near the drip-line [15]. Recently it has been shown [23]-[27] that the relativistic mean-field (RMF) plus BCS approach wherein the continuum has been replaced by the discrete single particle states for the calculation of the pairing energy provides an alternative fast approach to the relativistic Hartree-Fock-Bogoliubov (RHB) description [18], [22] of the drip-line nuclei.

Encouraged by the success of our RMF+BCS approach [23]-[27], and the impetus provided by the recent experimental developments, especially the measurements [1], [2], [3], we have employed it for the study of structure of even-even nuclei covering the whole periodic region up to the drip-lines to investigate the unusual proton and neutron magic numbers. For simplicity and transparency we have not considered the deformation degree of freedom. Indeed, by using such an approach we intend to utilize the advantage one has in the analysis of results in terms of spherical single particle wave functions. This is especially true for the understanding of shell closures and magicity, and behavior of the single particle states near the Fermi surface. Similarly, within such a framework contributions of neutron and proton single particle states to the density profiles, pairing gaps, total pairing energy etc. which are also equally important in the study of shell closures can be demonstrated with clarity. These aspects of the spherical framework indeed make this approach very useful especially for the study of poorly understood exotic nuclei. Nevertheless, we eventually compare our results with those of the RMF calculations including deformation [29], in particular for the magic nuclei to check if these nuclei persist to be spherical due to the proton and neutron shell closures.

This paper has been organized as follows. In Sec.II, a brief description of the relativistic mean-field model [15], [23] has been given. Section III has been devoted to the discussion of our results obtained with the TMA force parametrization. As a representative example from amongst the extensive calculations, we describe and analyze the results of our calculations for the chain of Si isotopes. This is followed by a brief description of the main results of similar analyzes for other nuclei exhibiting unusual shell closures and magicity. Finally Sec.IV provides a summary of our results and conclusions.

II. Relativistic Mean Field Model

Our RMF calculations have been carried out using the model Lagrangian density with nonlinear terms both for the σ and ω mesons along with the TMA parametrization as described in detail in Refs. [15], [23],

$$\mathcal{L} = \bar{\psi}[\imath\gamma^{\mu}\partial_{\mu} - M]\psi$$

G. Saxena is with the Department of Physics, Government Women Engineering College, Ajmer-305002, INDIA. e-mail: (gauravphy@gmail.com).
D. Singh and M. Kaushik are with Department of Physics, University of Rajasthan, Jaipur 302006, INDIA
Manuscript received ; revised.

$$+\frac{1}{2}\,\partial_\mu\sigma\partial^\mu\sigma - \frac{1}{2}m_\sigma^2\sigma^2 - \frac{1}{3}g_2\sigma^3 - \frac{1}{4}g_3\sigma^4 - g_\sigma\bar{\psi}\sigma\psi$$
$$-\frac{1}{4}H_{\mu\nu}H^{\mu\nu} + \frac{1}{2}m_\omega^2\omega_\mu\omega^\mu + \frac{1}{4}c_3(\omega_\mu\omega^\mu)^2 - g_\omega\bar{\psi}\gamma^\mu\psi\omega_\mu$$
$$-\frac{1}{4}G^a_{\mu\nu}G^{a\mu\nu} + \frac{1}{2}m_\rho^2\rho^a_\mu\rho^{a\mu} - g_\rho\bar{\psi}\gamma_\mu\tau^a\psi\rho^{\mu a}$$
$$-\frac{1}{4}F_{\mu\nu}F^{\mu\nu} - e\bar{\psi}\gamma_\mu\frac{(1-\tau_3)}{2}A^\mu\psi\ ,$$

where the field tensors H, G and F for the vector fields are defined by

$$\begin{aligned} H_{\mu\nu} &= \partial_\mu\omega_\nu - \partial_\nu\omega_\mu \\ G^a_{\mu\nu} &= \partial_\mu\rho^a_\nu - \partial_\nu\rho^a_\mu - 2g_\rho\,\epsilon^{abc}\rho^b_\mu\rho^c_\nu \\ F_{\mu\nu} &= \partial_\mu A_\nu - \partial_\nu A_\mu\ , \end{aligned}$$

and other symbols have their usual meaning. As usual these RMF calculations have been performed assuming 'no-sea' treatment [14] which amounts to neglecting the effects of the Dirac Sea.

Based on the single-particle spectrum calculated by the RMF described above, we perform a state dependent BCS calculations [30], [31]. As we already mentioned, the continuum is replaced by a set of positive energy states generated by enclosing the nucleus in a spherical box. Thus the gap equations have the standard form for all the single particle states, i.e.

$$\Delta_{j_1} = -\frac{1}{2}\frac{1}{\sqrt{2j_1+1}}\sum_{j_2}\frac{\left\langle (j_1{}^2)\,0^+\,|V|\,(j_2{}^2)\,0^+\right\rangle}{\sqrt{\left(\varepsilon_{j_2}-\lambda\right)^2+\Delta^2_{j_2}}} \times\sqrt{2j_2+1}\ \Delta_{j_2} \qquad (1)$$

where ε_{j_2} are the single particle energies, and λ is the Fermi energy, whereas the particle number condition is given by $\sum_j (2j+1)v_j^2 = \mathrm{N}$. In the calculations we use for the pairing interaction a delta force, i.e., V = -$\mathrm{V}_0\delta(r)$ with the same strength V_0 for both protons and neutrons. The value of the interaction strength V_0 = 350 MeV fm^3 was determined in Ref. [23], [24] by obtaining a best fit to the binding energy of Ni isotopes. We use the same value of V_0 for our present studies of isotopes of other nuclei as well. Apart from its simplicity, the applicability and justification of using such a δ-function form of interaction has been recently discussed in Refs. [10], whereby it has been shown in the context of HFB calculations that the use of a delta force in a finite space simulates the effect of finite range interaction in a phenomenological manner (see also [32] and [33] for more details). The pairing matrix element for the δ-function force is given by

$$\left\langle (j_1{}^2)\,0^+\,|V|\,(j_2{}^2)\,0^+\right\rangle = -\frac{V_0}{8\pi}\sqrt{(2j_1+1)(2j_2+1)}\ I_R \qquad (2)$$

where I_R is the radial integral having the form

$$I_R = \int dr\frac{1}{r^2}\left(G^\star_{j_1}G_{j_2} + F^\star_{j_1}F_{j_2}\right)^2 \qquad (3)$$

Here G_α and F_α denote the radial wave functions for the upper and lower components, respectively, of the nucleon wave function expressed as

$$\psi_\alpha = \frac{1}{r}\begin{pmatrix} i\ G_\alpha\ \mathcal{Y}_{j_\alpha l_\alpha m_\alpha} \\ F_\alpha\,\sigma\cdot\hat{r}\ \mathcal{Y}_{j_\alpha l_\alpha m_\alpha}\end{pmatrix}\ , \qquad (4)$$

and satisfy the normalization condition

$$\int dr\,\{|G_\alpha|^2 + |F_\alpha|^2\} = 1 \qquad (5)$$

In Eq. (5) the symbol $\mathcal{Y}_{jlm}$ has been used for the standard spinor spherical harmonics with the phase i^l. The coupled field equations obtained from the Lagrangian density in (1) are finally reduced to a set of simple radial equations [14] which are solved self consistently along with the equations for the state dependent pairing gap Δ_j and the total particle number N for a given nucleus.

III. Results and Discussion

In what follows we first discuss, as a representative example, our RMF results for the entire chain of $^{22-48}$Si isotopes, the predicted lightest and heaviest bound isotopes amongst these being ^{22}Si and ^{48}Si, respectively. Interestingly, the results for the proton pairing gaps, their pairing energy, proton single particle spectra as well as the proton density profiles show that the proton shell closure occurs for all the isotopes of Si consistently at Z=14. The fully occupied proton sp states being $1s_{1/2}$, $1p_{3/2}$, $1p_{1/2}$, and $1d_{5/2}$. However, the lightest isotope ^{22}Si is found to be just bound. Indeed, for this proton rich isotope due to large coulomb interaction the proton sp potential becomes quite shallow and the proton Fermi level, having energy ϵ_f = 0.58 MeV, lies just above the continuum threshold whereas the last bound proton sp $1d_{5/2}$ state is bound just by 0.71 MeV. The pairing energy contribution from protons for all the isotopes indeed remains zero throughout. This unusual magicity at Z=14 is found to be due to large gap between the proton sp state $1d_{5/2}$ and the other two sp states $1d_{3/2}$ and the $2s_{1/2}$ in the s-d shell. This conclusion is also supported by rapidly decreasing proton density for all the isotopes within a short radial distance.

In order to demonstrate the probable neutron shell closures as well in these isotopes, and hence identify the doubly magic nuclei, we have shown in Fig. 1 the variation in the pairing energy from neutrons (protons contribution being zero for all the Si isotopes), the two-neutron separation energy, and the neutron single particle (sp) energy for the entire chain of Si isotopes as a function of neutron number N. As seen from the upper panel in Fig. 1 the neutron pairing energy also vanishes for each of the Si isotopes with neutron number N = 8, 14, 20, 28 and 34 indicating the shell closures for both the protons and neutrons. Thus for the proton magic number at Z = 14, apart from the traditional neutron shell closures at N = 8, 20 and 28, new shell closures appear at N = 14 and 34 making the isotopes ^{22,28,34,42,48}Si doubly magic.

These sp shell structures as revealed by the neutron dependence of the pairing energy are also exhibited in the variation of two-neutron separation energies, S_{2n}, shown in the middle panel of Fig. 1. An abrupt decrease in the S_{2n} value for the isotopes with neutron magic number is evidently seen. Beyond N = 34, S_{2n} becomes negative and thus we reach the drip-line at N = 34 for Z = 14. An extensive study of isotones also confirms the proton shell closure at Z = 14. Indeed, from the neutron sp structure as seen in the lower panel of Fig. 1, we find that the sp energy gaps as found for Z=14 are

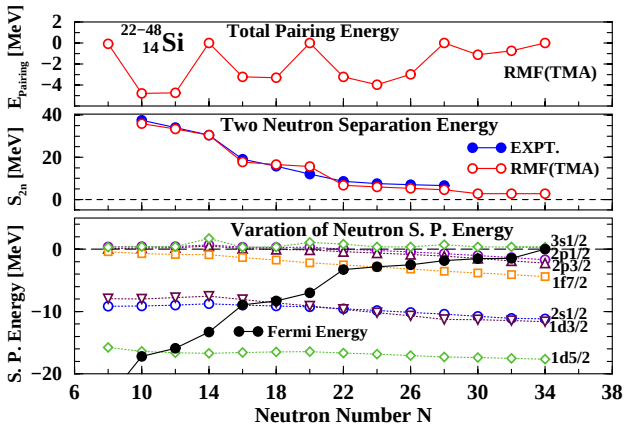

Fig. 1. RMF+BCS results for the Si isotopes showing the neutron number N dependence of the (i) total pairing energy (upper panel), (ii) two neutron separation energy and its comparison with the available experimental data [34] (middle panel), and (iii) relevant neutron single particle energy spectrum along with the position of neutron Fermi energy depicted by solid circles and connected by solid line (lower panel).

also maintained for the neutron number N = 14. Further, it is expected from the isospin symmetry [9] considerations that the mirror nuclei having N = 14 and Z = 8, 20, 28, and 34 should also exhibit similar shell closures. Calculated results show that of these the bound mirror nuclei ^{22}O and ^{34}Ca are indeed doubly magic, whereas the remaining ^{42}Ni and ^{48}Se are unbound due to excessively large Coulomb repulsion of protons in these neutron deficient nuclei.

Further, we want to point out, as can be seen from the middle plot depicting the separation energy in Fig. 1, that for the isotopes with N = 30 - 34 the S_{2n} value is rather small. The last neutrons in these nuclei fill in the sp states $2p_{3/2}$ and $2p_{1/2}$ which lie close to the Fermi level near the continuum threshold. Just above these two states lies the $3s_{1/2}$ state which remains in the continuum and does not come down to be bound even if further neutrons are added beyond N=34. This is due to the fact that it has no centrifugal barrier and its wave function is widely spread beyond the range of the potential. This fact consequently plays a crucial role in deciding the neutron drip line at N=34 and thus we have ^{48}Si as the heaviest bound isotope for the element Si. However, for the ^{44,46,48}Si isotopes the wave functions of the last neutrons, which occupy the low angular momentum sp states $2p_{3/2}$ and $2p_{1/2}$ with small centrifugal barrier have also considerable spread outside the potential region, albeit not to the extent the neutron $3s_{1/2}$ state mentioned above. Due to this these neutrons are somewhat loosely bound. Consequently, for these isotopes there occurs a sudden increase in the neutron rms radius as found in our calculations. Also, due to the fact that the last filled states for the ^{44,46,48}Si isotopes lie near the continuum threshold, these nuclei have small S_{2n} values. Moreover, since the sp states $2p_{3/2}$ and $2p_{1/2}$ have moderate sp energy gaps with respect to both the $1f_{7/2}$ and $3s_{1/2}$ sp states, we have the neutron number N = 34 as a magic number. A detailed study of the pairing interaction energy and the wave function of the single particle states shows that the neutron sp $2f_{5/2}$ state which lies in the continuum at around 1.9 MeV is a resonant state. However, as it lies at higher energy from the last filled states near the Fermi level its contribution to the pairing correlation energy is rather negligible. Nevertheless, it is worthwhile at this point to emphasize the role of the location of such a resonant $2f_{5/2}$ state and that of the $3s_{1/2}$ sp state: in fact had this resonant state been at lower energy its coupling to the nearby bound sp states, for example $2p_{1/2}$ and $2p_{3/2}$, due to pairing interaction would be large. This would result in further addition of neutrons to the resonant state and thus an extension in the position of the neutron drip line beyond N=34. Moreover, due to this role of accommodating more neutrons to keep the system bound, the resulting potential becomes rather favorable to bring down the $3s_{1/2}$ state very close to the Fermi level and couple with the bound states to get partially or fully occupied. A filling in of such an s-state lying at the threshold of the continuum gives rise to a halo formation in nuclei. Such a role of sp resonant state combined with that of the position of an s-state has been shown earlier [23] to give rise to a large halo formation in the extremely neutron rich Ca isotopes.

The results described above are further supported by the calculated proton and neutron density distributions wherein it is seen that the densities fall off rapidly for the closed shell ^{22,28,34,42,48}Si isotopes as compared to that for other isotopes having tails of neutron density extending beyond the potential region. Also the calculated radii are found to be in agreement with the available measurements [35], [36], [37]. Thus, the important prediction of these calculations is that in addition to the isotopes ^{28,34,42}Si being doubly magic, ^{22}Si and ^{48}Si isotopes are also doubly magic. The isotope ^{48}Si lies on the neutron drip-line, whereas ^{22}Si falls on the proton drip-line. These two isotopes, respectively, constitute examples of neutron and proton rich doubly magic drip-line nuclei. So far the heaviest isotope of Si which has been experimentally observed is ^{43}Si and it would be interesting to look for the experimental confirmation of heavier isotopes, especially the doubly magic ^{48}Si at the neutron drip-line.

In order to check the possible dependence and sensitivity of results on the force parametrization, we have also carried out these calculations employing other popular RMF parameterizations, the NL3 and NLSH as given in detail in Refs. [18] and [19], respectively. A comparison of the results for the Si isotopes shows that these forces (the TMA, NL3 and NLSH parameterizations) essentially yield similar results. Indeed the results for the separation energy, proton and neutron radii, density profiles and drip lines etc. are almost identical for all the Si isotopes. The same is found to be true for the proton and neutron sp spectra excepting a small deviation in the NL3 results for the proton sp spectrum of ^{22}Si and that for the neutron sp spectrum of ^{42}Si as compared to those of TMA and NLSH results. To elaborate, whereas the TMA and NLSH results show shell closures for both protons and neutrons in ^{22}Si and ^{42}Si, the NL3 results indicate that ^{22}Si has shell closure only for the neutrons, and similarly ^{42}Si exhibits shell closure only for protons. However, from the detailed study of the pairing energy, sp pairing gaps and occupancies of the sp levels, it is observed that in fact the deviation from the shell closures in these two nuclei for the NL3 force is rather small.

Our findings of unusual magic numbers N=34 at neutron drip-line and Z=14 at proton drip-line are in agreement with the systematic RMF calculations including deformation in Ref. [29] which shows that nuclei ^{22,48}Si have spherical shape. Experimental measurement for ^{22,48}Si isotope would be extremely interesting in order to test the drip-line as well as the these new unusual shell closures.

The above encouraging description of the entire chain of Si isotopes employing the spherical framework provided us with strong motivation to extend these investigations to the entire chart of the nuclei up to the drip-lines, especially, to study in detail the occurrence of shell closures. As has been demonstrated above, these features of nuclei are primarily governed by the sp structures, the location of possible resonant states, coupling due to the pairing interaction between the bound and unbound states, especially the resonant states near the Fermi level, and changes in the total number of protons and neutrons which in turn govern the shape of proton and neutron potentials. Again, as in the case of Si isotopes, these studies have also been carried out in terms of pairing energy, two neutron and two proton separation energies, (S_{2n} and S_{2p}), single particle proton and neutron spectra, rms radii and density distribution profiles for the protons and neutrons to obtain the magic numbers.

As an illustration Fig. 2 shows the two-neutron separation energy S_{2n} with increasing neutron number N. The various curves in the figure connect the nuclei with the same isospin component T_Z = (N-Z)/2 ranging from -2 to 12. In this figure, the results for nuclei with neutron number N only up to 54 have been displayed. Plots of S_{2n} covering nuclei with higher N, and analogous plots for the two-proton separation energy S_{2p} with increasing Z values exhibit similar characteristics and have not been displayed here in order to save space. In Fig. 2, and in similar plots for heavier nuclei, a sudden decrease in the two-neutron separation energies S_{2n} is clearly seen at the major shell closures corresponding to traditional neutron magic numbers N = 8, 20, 28, 50, 82 and 126. Analogously, a decrease is observed in the two-proton separation energies S_{2p} (not shown here) at the traditional proton magic numbers Z = 8, 20, 28, 50 and 82. These major neutron and proton shells are seen generally to persist well into regions belonging to proton rich as well as neutron rich nuclei while approaching the drip-lines. For these magic numbers the chains of bound isotopes and isotones are relatively large. Such magic numbers may be termed as strong magic numbers. However, there are instances, especially for neutron rich cases, whereby a major shell structure is weakened and the associated magic number disappears with the emergence of a new magic number. For example, the present approach yields that for the neutron rich Ca isotopes the magicity for N = 50 disappears, while N = 40 becomes a new magic number. This is due to appreciable gap between the $1f_{5/2}$ and $1g_{9/2}$ as the $1g_{9/2}$ state is shifted upward closer to the 3s - 2d shells. Indeed as seen in Fig. 2 the neutron number N = 40 shows magicity for other nuclei corresponding to curves for T_Z values ranging from 7 to 12. Thus N = 40 is found to be a magic number for the nuclei ^{56}S, ^{58}Ar, ^{60}Ca, ^{62}Ti, ^{64}Cr and ^{66}Fe with Z values between 16 and 26. These predictions of magicity for N=40 are found

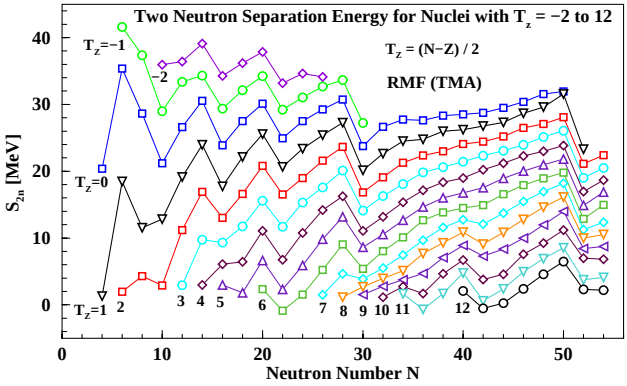

Fig. 2. Calculated results obtained in the RMF+BCS approach showing the variation of two-neutron separation energy S_{2n} with increasing neutron number N. The lines connect the nuclei with same isospin value T_Z = (N-Z)/2 = -2, -1, 0, 1, 2, ...10, 11 and 12. At the magic numbers a sudden decrease in the separation energy is evidently seen.

to be consistent also with the results of Ref. [29] showing no deformation for these nuclei.

In a similar manner, we find that nuclei in different regions of the periodic table lying between the line of beta-stability and the drip-lines exhibit shell closures at other N or/and Z values due to the variations in the neutron and proton single particle structures with changing N or/and Z values. These results have been collected in Table 1. For the proton number Z given in column 1 of the table, column 2 provides the neutron number of all those isotopes which are found to be bound. All bound isotopes may or may not be proton magic, and hence, columns 3 gives the isotopes for which Z is a magic number, whereas column 4 provides explicitly the doubly magic isotopes. Analogously, column 5 lists the neutron number N for which the bound isotones are listed in column 6 which gives their Z values. Again, all these bound isotones may not necessarily be neutron magic nuclei, and hence, column 7 provides the isotones for which N is a magic number, and column 8 gives the doubly magic isotones.

Indeed, besides the traditional magic numbers, the lightest nuclei show magicity at Z = 6 for neutron number from N = 4 to N = 16, and analogously at N = 6 for proton number from Z = 2 to Z = 8 as has been listed in Table 1. It appears that the magicity at Z = 6 and N = 6, and similarly for several other Z and N values up to Z or N = 34 as seen in Table 1, holds good in a symmetric manner for the neutron rich and proton rich nuclei, respectively, though due to Coulomb repulsion very rich proton nuclei are found to be unbound in comparison to neutron rich cases. The sp structure shows that in lighter nuclei the occurrence of these magic numbers is caused due to the increased spacing between the $1p_{3/2}$ and $1p_{1/2}$ states. Amongst these, the nuclei ^{8}He, ^{12}C and ^{14}O etc. appear to be doubly magic. Moving up, we find Z = 14 to be a magic number for all the isotopes with even N values ranging between 8 and 34. Out of these the isotopes ^{22,28,34,42,48}Si are predicted to be doubly magic as described in detail in the context of Si isotopes above. Similarly, N = 14 is found to be a magic number for nuclei with even Z values between 8 and

TABLE I
PROTON MAGIC, NEUTRON MAGIC AND DOUBLY MAGIC NUCLEI OBTAINED FROM RMF+BCS CALCULATIONS FOR EVEN-EVEN ISOTOPES ($Z \leq 114$) AND ISOTONES ($N \leq 126$) USING THE TMA INTERACTION [15]. COLUMN 2 GIVES THE RANGE OF BOUND ISOTOPES FOR THE PROTON NO. Z IN COLUMN 1. OUT OF THE BOUND ISOTOPES IN COLUMN 2, THOSE SHOWING ONLY PROTON MAGICITY ARE GIVEN IN COLUMN 3, AND THOSE SHOWING BOTH PROTON AND NEUTRON MAGICITY (DOUBLY MAGIC) ARE SHOWN IN COLUMN 4. THE NEXT FOUR COLUMS PROVIDE ANALOGOUS RESULTS FOR NEUTRON NO. N GIVEN IN COLUMN 5. THESE MAGIC NUMBERS ARE PREDICTED ON THE BASIS OF TWO-NEUTRON, TWO-PROTON SEPARATION ENERGY, PAIRING ENERGIES FOR PROTONS AND NEUTRONS, PAIRING GAPS, SINGLE PARTICLE SPECTRA, DENSITY PROFILES FOR THE PROTON AND NEUTRON DISTRIBUTIONS, AND THEIR RMS RADII.

Proton no. Z	Range of bound isotopes with neutron no. N	Magic and doubly magic isotopes		Neutron no. N	Range of bound isotones with proton no. Z	Magic and doubly magic isotones	
		Range of proton magic isotopes with neutron no. N	Doubly magic isotopes with neutron no. N			Range of neutron magic isotones with proton no. Z	Doubly magic isotones with proton no. Z
2	2 - 6	2 - 6	2, 6	2	2	2	2
6	4 - 16	4 - 16	6, 8, 16	6	2 - 8	2 - 8	2, 6, 8
8	4 - 20	4 - 20	6, 8, 14, 16, 20	8	4 - 14	4 - 14	6, 8, 14
14	8 - 34	8 - 34	8, 14, 20, 28, 34	14	6 - 20	8 - 20	8, 14, 20
16	10 - 40	10 - 12		16	6 - 20	6 - 10	6, 8
20	14 - 50	14 - 50	14, 20, 28, 40	20	8 - 28	8 - 28	8, 14, 20, 28
28	20 - 70	20 - 70	20, 28, 50, 70	28	12 - 30	14 - 30	14, 20, 28
34	32 - 82	80 - 82	82	34	12 - 38	12 - 16	14
				40	16 - 44	16 - 26	20
50	46 - 126	46 - 126	50, 82, 126	50	20 - 50	22 - 50	28, 50
				70	26 - 62	26 - 32	28
82	96 - 184	96 - 130	126	82	32 - 72	32 - 72	34, 50
				112	40 - 90	40 - 44	
				126	48 - 94	48 - 88	50, 82

20 as can be seen in Table 1 and also in Fig. 2. Moreover, N = 14 with Z = 8, 14 and 20 provides doubly magic nuclei ^{22}O, ^{28}Si and ^{34}Ca. Next we find that Z = 16 is a proton magic number for the proton rich isotopes $^{26-28}$S as shown in Table 1. Similarly, our calculations predict the appearance of N = 16 as a magic number for the neutron rich nuclei ^{22}C, ^{24}O and ^{26}Ne as is also seen in Fig. 2. Moreover, out of these three, ^{22}C and ^{24}O are observed to be doubly magic nuclei. The magicity at N or Z = 16 results due to increased spacing of the sp energy levels $2s_{1/2}$ and $1d_{5/2}$ from the $1d_{3/2}$ sp state. Further up, calculations show magicity at Z = 34 for the neutron rich isotopes ^{114,116}Se. Out of these two, the isotope ^{116}Se is found to be doubly magic. Similarly, N = 34 is found to be a magic number for neutron rich nuclei with Z values ranging from 12 to 16 due to the large spacing of neutron $2p_{3/2}$ and $2p_{1/2}$ states from the $1f_{5/2}$ state. With Z = 14 this yields a doubly magic nucleus ^{48}Si. Thus, interesting results in the table are the prediction of unusual proton magic numbers at Z = 6, 14, 16, 34, and neutron magic numbers at N = 6, 14, 16, 34, 40, 70, 112, in addition to the traditional magic numbers. In contrast to neutron case, no proton magic numbers are predicted at Z = 40, 70 and 112.

In order to check the force parameter dependence of these results, we repeated these RMF+BCS calculations using the NL3 and NLSH parameters [18], [19]. The calculated results, apart from the minor details, remained essentially close to those obtained using the TMA force parameters. Calculations [38], [39] similar to that of Ref. [29] including the deformation degree of freedom, however, show that most of the isotopes or isotones with traditional magic numbers are not deformed, and some of isotopes of C, Si etc are actually deformed. Nevertheless, the main conclusions of our results remain unchanged.

For the Oxygen isotopes the calculations show that ^{14,16,22,24}O are doubly magic nuclei. The isotopes ^{26,28}O are found to be bound which is at variance with the experimental data [34], though consistent with the results of other mean field calculations including those carried out with deformation degree of freedom [29]. This discrepancy with respect to measurements needs separate investigations.

IV. CONCLUSION

Inspired by the recent experiments [1], [2], [3] indicating unusual doubly magic nucleus ^{24}O which lies just at the neutron drip-line and encouraged by the success of our relativistic mean-field (RMF) plus state dependent BCS approach for the description of the ground state properties of the drip-line nuclei [23], [25], we have further employed this approach, across the entire periodic table, to explore the unusual shell closures. The Lagrangian density with nonlinear terms for the σ and ω mesons along with the TMA force parameters [15] has been employed for the purpose. State dependent BCS calculations employing a delta function interaction with the same interaction strength throughout have been performed for the pairing correlation energy. The calculated results comprising the systematics for the pairing energy, pairing gaps, two-neutron and two-proton separation energies have been analyzed to predict the possible magic numbers.

The results, in particular, for the entire chain of Si isotopes show that the proton number Z=14 represents a shell closure throughout up to the neutron drip-line which is found to be at N=34. More interestingly, it has been found that the isotopes ^{22,28,34,42,48}Si are doubly magic indicating persistence of the neutron shell closure at N=8, 14, 20, 28 and 34. These findings, especially the fact that the heaviest and highly neutron rich ^{48}Si nucleus is doubly magic need experimental confirmation.

Our calculations, especially in the case of neutron rich nuclei, show that the interplay of (i) variation in energy of the proton and neutron sp states due to change in the number of protons and neutrons, and (ii) the position of resonant states greatly influences the shell closures, and hence, the magicity in nuclei. The neutron rich Si isotopes, ^{44,46,48}Si, provide example of loosely bound isotopes near the drip-line due to filling in of the low angular momentum sp states $2p_{3/2}$ and $2p_{1/2}$. Present calculations predict the unusual proton magic numbers at Z = 6, 14, 16, 34, and unusual neutron magic numbers at N = 6, 14, 16, 34, 40, 70, 112. These results are found to be consistent with the experimental systematics [34] of two-proton and two-neutron separation energies, S_{2p} and S_{2n}, respectively.

Acknowledgment

Authors would like to thank Prof. H. L. Yadav for his kind hospitality and guidance while visiting, Banaras Hindu University, Varanasi, INDIA. The authors are indebted to Dr. L. S. Geng, RCNP, Osaka, Japan for valuable correspondence.

References

[1] Robert V. F. Janssens, Nature 459 (2009) 1069.
[2] R. Kanungo, *et al*., Phys. Rev. Lett. 102 (2009) 152501.
[3] C. R. Hoffman, *et al*., Phys. Lett. B 672 (2009) 17.
[4] I. Tanihata, J. Phys. G 22 (1996) 157;
I. Tanihata *et al.*, Phys. Lett. B 512 (2001) 261.
[5] A. Ozawa, T. Kobayashi, T. Suzuki, K. Yoshida and I. Tanihata, Phys. Rev. Lett. 84 (2000) 5493;
A. Ozawa *et al.*, Nucl. Phys. A 709 (2002) 60.
[6] A. Jensen, K. Riisagar, D. V. Fadarov and E. Garrido, Rev. Mod. Phys. 76 (2004) 215, and reference therein;
A. S. Jensen and K. Riisager, Phys. Lett. B 480 (2000) 39;
P. G. Hansen and A. S. Jensen, Annu. Rev. Nucl. Part. Sci. 45 (1995) 591.
[7] S. Dasgupta, I. Mazumdar and V.S. Bhasin, Phys. Rev. C 50 (1994) 551(R)
[8] G. Bertsch, H. Esbensen and A. Sustich, Phys. Rev. C 42 (1990) 758.
[9] T. Otsuka *et al*., Phys. Rev. Lett. 87 (2001) 082502.
[10] J. Dobaczewski *et al*., Phys. Rev. C 53 (1996) 2809.
[11] M. Grasso *et al*., Phys. Rev. C 64 (2001) 064321.
[12] B. D. Serot and J. D. Walecka, Adv. Nucl. Phys. 16 (1986) 1.
[13] P. G. Reinhard, Rep. Prog. Phys. 52 (1989) 439; and references therein.
[14] P. G. Reinhard, M. Rufa, J. Marhun, W. Greiner and J. Friedrich, Z. Phys. A 323 (1986) 13.
[15] Y. Sugahara and H. Toki, Nucl. Phys. A 579 (1994) 557.
[16] R. Brockman and H. Toki, Phys. Rev. Lett. 68 (1992) 3408.
[17] P. Ring, Nucl. Part. Phys. 24 (1998) 1467.
[18] G. A. Lalazissis, D. Vretenar and P. Ring, Phys. Rev. C 57 (1998) 2294.
[19] M. M. Sharma, M. A. Nagarajan and P. Ring, Phys. Lett. B 312 (1993) 377.
[20] M. Del Estal, M. Contelles, X. Vinas and S. K. Patra, Phys. Rev. C 63 (2001) 044321.
[21] J. Meng, Phys. Rev. C 57 (1998) 1229.
[22] J. Meng, H. Toki, J. Y. Zeng, S. Q. Zhang and S. G. Zhou, Phys. Rev. C 65 (2002) 041302(R).
[23] H. L. Yadav, M. Kaushik and H. Toki, Int. Jour. Mod. Phys E 13 (2004) 647.
[24] H. L. Yadav, S. Sugimoto and H. Toki, Mod. Phys. Lett. A 17 (2002) 2523.
[25] M. Kaushik, D. singh and H. L. Yadav, Acta Phys. Slov. 5 No. 2 (2005) 181.
[26] G. Saxena, D. singh, H. L. Yadav, A. Haga and H. Toki, Modern Physics Letters A 23 (2008) 2589.
[27] D. Singh and G. Saxena, Int. Jour. Mod. Phys E, Vol. 21, No. 9, (2012) 1250076.
[28] B. G. Todd-Rutel, J. Piekarewicz and P. D. Cottle, Phys. Rev. C 69 (2004) 021301.
[29] L. S. Geng, Ph. D. Thesis, RCNP, Osaka University, Osaka, (2005);
L. S. Geng, H. Toki, S. Sugimoto and J. Meng, Prog. Theor. Phys. 110 (2003) 921.
[30] A. M Lane, *Nuclear Theory* (Benjamin, 1964).
[31] P. Ring and P. Schuck, *The Nuclear many-body Problem* (Springer, 1980).
[32] G. F. Bertsch and H. Esbensen, Ann. Phys. (N.Y.) 209 (1991) 327.
[33] A. B. Migdal, *Theory of Finite Fermi Systems and Applications to Atomic Nuclei* (Interscience, New York, 1967).
[34] G. Audi, A. H. Wapstra and C. Thibault, Nucl. Phys. A 729 (2003) 337.
[35] G. Fricke *et al.*, Phys. Rev. 45 (1992) 80.
[36] H. de Vries, C. W. de Jager, and C. de Vries, At. Data Nucl. Data Tables 36 (1987) 495.
[37] C. J. Batty, E. Friedman, H. J. Gils and H. Rebel, Adv. Nucl. Phys. 19 (1989) 1.
[38] M. M. Sharma, S. Mythili and A. R. Farhan, Phys. Rev C 59 (1998) 1379.
[39] Z. Ren, Z. Y. Zhu, Y. H. Cai and Gongou Xu, Nucl. Phys. A 605 (1996) 75.